

## Interdigitated Residues within a Small Region of VP16 Interact with Oct-1, HCF, and DNA

JIANN-SHIUN LAI<sup>1,2†</sup> AND WINSHIP HERR<sup>1\*</sup>

*Cold Spring Harbor Laboratory, Cold Spring Harbor, New York 11724,<sup>1</sup> and Graduate Program in Genetics, State University of New York at Stony Brook, Stony Brook, New York 11794<sup>2</sup>*

Received 18 February 1997/Returned for modification 23 March 1997/Accepted 3 April 1997

Upon infection, the herpes simplex virus (HSV) activator of immediate-early (IE) gene transcription VP16 forms a multiprotein-DNA complex with two cellular proteins, Oct-1 and HCF. First, VP16 associates with HCF independently of DNA, and this association stimulates subsequent association with Oct-1 on the DNA target of VP16 activation, the TAATGARAT motif found in HSV IE promoters. We have analyzed the involvement of VP16 residues lying near the carboxy-terminal transcriptional activation domain of VP16 in associating with HCF, Oct-1, and DNA. To assay VP16 association with HCF, we developed an electrophoretic mobility retardation assay in which HCF is used to retard the mobility of a hybrid VP16-GAL4 DNA-binding domain fusion protein bound to a GAL4 DNA-binding site. Analysis of an extensive set of individual and combined alanine substitutions over a 61-amino-acid region of VP16 shows that, even within a region as small as 13 amino acids, there are separate residues involved in association with either HCF, DNA, or Oct-1 bound to DNA; indeed, of two immediately adjacent amino acids in VP16, one is important for DNA binding and the other is important for HCF binding. These results suggest that a small region in VP16 is important for linking in close juxtaposition the four components of the VP16-induced complex and support the hypothesis that the structure of the Oct-1-VP16 interaction in this complex is similar to that formed by the yeast transcriptional regulatory proteins MAT $\alpha$ 1 and MAT $\alpha$ 2. We propose that HCF stabilizes this Oct-1-VP16 interaction.

In mammalian cells, transcription is frequently regulated by the coordinated and specific assembly of transcription factors on individual *cis*-regulatory sites within a promoter. One such coordinated and specific multiprotein-DNA assembly is the herpes simplex virus (HSV) VP16-induced complex (for reviews, see references 23 and 32). This complex is formed among four components: two cellular proteins (the POU domain transcription factor Oct-1 and the host cell factor HCF), the HSV virion protein VP16, and *cis*-regulatory sites in HSV immediate-early (IE) promoters that conform to the sequence motif TAATGARAT (R = purine). Upon HSV infection, VP16 is released from the virion into the cell, whereupon it first associates with HCF to form a DNA-independent heterodimeric complex (15, 18, 27, 40). This heterodimeric complex can then form a DNA-dependent VP16-induced complex with Oct-1, but not the closely related POU domain protein Oct-2, on TAATGARAT sites (for a review, see reference 13).

The two cellular factors in the VP16-induced complex, Oct-1 and HCF, are not known to associate with one another in the absence of VP16. Oct-1 is a broadly expressed transcription factor that recognizes with high affinity the octamer sequence ATGCAAAT. Oct-1 recognizes DNA through its POU domain, a bipartite DNA-binding domain consisting of an amino-terminal POU-specific domain and a carboxy-terminal POU homeodomain joined by a hypervariable and flexible linker (for a review, see reference 13). HCF, also referred to as C1 (16), VCAF (40), and CFF (15), is required for cell cycle progression (7) and comprises a series of noncovalently associated amino-terminal and carboxy-terminal polypeptides that arise by proteolytic processing of a 300-kDa precursor protein (17, 36–38).

The one viral factor in this complex, VP16 (also referred to as Vmw65 and  $\alpha$ TIF), is a multifunctional protein of 490 amino acids that is both an essential structural component of the HSV virion and an activator of HSV IE gene transcription (for reviews, see references 23 and 32). VP16 contains two functionally distinct regions: a 340-amino-acid amino-terminal region (residues 49 to 388) responsible for VP16-induced complex formation (8, 9, 33) and an acidic 80-amino-acid carboxy-terminal region responsible for activating IE gene transcription (4, 25, 33). Three different types of analyses, (i) mutagenesis (1, 9, 26, 27, 34, 35), (ii) use of peptides to either mimic (27) or inhibit (10, 11, 39) VP16 function, and (iii) protease sensitivity (11), have focused attention on the role of a small segment of VP16 lying near the transcriptional activation domain in directing VP16-induced complex formation.

In this study, we have systematically mutated residues (both individually and in combination) within this important region of VP16 and studied how these residues coordinate assembly of the VP16-induced complex, by measuring their effects on complete VP16-induced complex formation and individual interaction with HCF, DNA, and Oct-1 bound to DNA. Most of the mutations affected VP16 association with either HCF, DNA, or Oct-1 bound to DNA but rarely disrupted all three VP16 activities simultaneously. This pattern of selective disruption of VP16 activity within a small segment of VP16 suggests that this region of VP16 is critical for linking the four components of the VP16-induced complex together.

### MATERIALS AND METHODS

**Expression constructs and protein purification.** The wild-type glutathione *S*-transferase (GST)-VP16 $\Delta$ C *Escherichia coli* expression construct containing an HSV type 1 VP16 truncation lacking the carboxyl-terminal acidic activation domain (residues 5 to 412) has been described previously (37). For mutagenesis, an *f1* replication origin (12) was inserted into the unique *EcoRI* site of pET11c (28) to produce antisense single-stranded DNA. This pET11c derivative is referred to as pET11c.ori<sup>+</sup>(-)/VP16 $\Delta$ C. *E. coli* expression constructs of wild-type and mutant GST-GAL4-VP16 $\Delta$ C fusion proteins were obtained by inserting a

\* Corresponding author. Phone: (516) 367-8401. Fax: (516) 367-8454. E-mail: herr@cshl.org.

† Present address: Department of Biology, Massachusetts Institute of Technology, Cambridge, MA 02139.

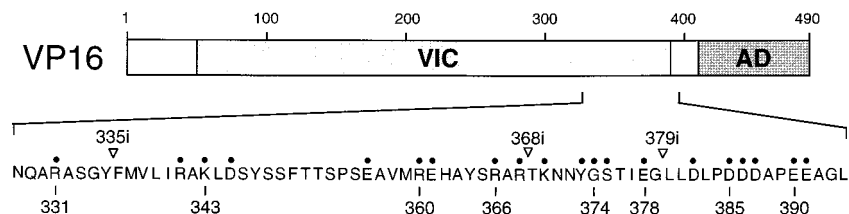


FIG. 1. Positions of amino acid substitutions within VP16 residues 331 and 391. A schematic of the 490-amino-acid VP16 protein with the amino acid sequence of residues 328 to 394 is shown. The regions required for VP16-induced complex formation (VIC; residues 49 to 388) and transcriptional activation (AD; residues 413 to 490) are stippled. The positions of the 335i, 368i, and 379i insertion mutations are indicated by arrowheads. Residues substituted in this study are marked by dots.

*SylI-XbaI* DNA fragment containing the coding sequences for the GAL4 DNA-binding domain (residues 1 to 94) into the unique *XbaI* site that lies between the GST- and VP16-coding sequences in the GST-VP16 fusion protein expression constructs. The wild-type GST-Oct-1 POU domain *E. coli* expression construct, pET11c.G.POU-1.ori<sup>+</sup>(-), containing human Oct-1 residues 280 to 439, has been described previously (20). The wild-type and variant GST-VP16 $\Delta$ C and GST-GAL4-VP16 $\Delta$ C and wild-type GST-Oct-1 POU domain fusion proteins were expressed and purified as previously described (20).

The wild-type VP16 mammalian expression construct pCGNVP16 contains the entire VP16-coding sequence (3). Mutant pCGNVP16 constructs were obtained by transferring the mutated VP16-coding sequences (residues 5 to 412) as a *SaI*I fragment from the GST-VP16 $\Delta$ C expression construct to the wild-type pCGNVP16 construct.

**Mutagenesis.** Mutations were created by oligonucleotide-directed mutagenesis as described previously (19). We used VP16 $\Delta$ C as the wild-type reference for the in vitro complex formation studies and as the substrate for mutagenesis. For each amino acid substitution mutation, a companion restriction site was either created or destroyed to serve as a marker for screening the mutations. The sequences created in the oligonucleotide-directed mutants are as follows: R331A, GCCggcGC (*SacII*<sup>+</sup>); 341A1a3, TgccGCGgGTTGGcCT (*SacII*<sup>+</sup>); R341A, TgcG GcCAA (*EaeI*<sup>+</sup>); K343A, GgccTTGGA (*SylI*<sup>+</sup>); D345A, GGctagcT (*NheI*<sup>+</sup>); E356A, TctGcaGC (*PstI*<sup>+</sup>); 360A1a2, AGGCcGTCATGgccGcAC (*SfiI*<sup>+</sup>); R360A, ATGgccGA (*EaeI*<sup>+</sup>); E361A, CGGGccCA (*ApaI*<sup>+</sup>); 366A1a3, Cgc CGCGgcTACGgcAA (*SacII*<sup>+</sup>); R366A, CtctgcaGC (*PstI*<sup>+</sup>); R368A, CagcTA (*AluI*<sup>+</sup>); K370A, ACGgccAA (*EaeI*<sup>+</sup>); Y373A, TgcCGGcT (*NaeI*<sup>+</sup>); G374A, TAtGcaTC (*NsiI*<sup>+</sup>); S375A, GGgCTACC (*AccI*<sup>-</sup>); E378A, CGccGGCC (*NaeI*<sup>+</sup>); D382A, CGcTCT (*MboI*<sup>+</sup>); 385A1a3, GGcTgcaGCcCG (*PstI*<sup>+</sup>); and 390A1a2, CGcAGcAGcTGGcC (*PvuII*<sup>+</sup>). The uppercase letters represent the wild-type sequences, and the lowercase letters represent mutations; the boldface letters encode the missense mutation; and the created (+) or destroyed (-) restriction sites are underlined and identified in parentheses. Each mutation was verified by DNA sequence analysis. The insertion mutations 335i (R335), 368i (R369), and 379i (in14) have been described previously (1, 35).

**Electrophoretic mobility retardation assays.** Two different probes, containing either a single (OCTA<sup>+</sup>)TAATGARAT site (20) or a synthetic high-affinity GAL4-binding site (called G17M [29]), were used in the electrophoretic mobility retardation assays; they were prepared by PCR as described previously (2). Human HeLa cell-derived HCF and Oct-1 were provided by a single fraction (the wheat germ agglutinin [WGA] Oct-1+HCF fraction) purified by WGA chromatography (37) (a gift of A. Wilson).

For the complete VP16-induced complex assay, purified GST-VP16 $\Delta$ C protein (~20 ng), the WGA Oct-1+HCF fraction (~1  $\mu$ g), and the (OCTA<sup>+</sup>)TAATGARAT DNA probe were mixed in a 10- $\mu$ l reaction mixture, and the reactions were analyzed by electrophoresis through a 4% polyacrylamide (39:1 acrylamide/bisacrylamide) gel as previously described (20). For the VP16-HCF interaction assay, purified GST-GAL4-VP16 $\Delta$ C (~5 ng) alone or with added WGA Oct-1+HCF fraction (~100 ng) was mixed in a 10- $\mu$ l reaction mixture containing 10 mM Tris (pH 8.0), 60 mM NaCl, 5 mM MgCl<sub>2</sub>, 20  $\mu$ M ZnSO<sub>4</sub>, 1 mM dithiothreitol, 1 mM EDTA, 0.05% Nonidet P-40, 1% glycerol, 2% Ficoll 400, 10 ng of sonicated salmon sperm DNA, 75 ng of poly(dI-dC), 3% fetal calf serum, and 20,000 cpm of G17M GAL4 probe. After incubation at 30°C for 30 min, the reaction samples were analyzed by electrophoresis through a 4% polyacrylamide gel under the same conditions as for the VP16-induced complex assay.

For VP16-DNA and VP16-Oct-1-DNA assays, high (~1  $\mu$ g) and intermediate (~0.2  $\mu$ g) concentrations, respectively, of GST-VP16 $\Delta$ C were used. In addition, wild-type GST-Oct-1 POU domain protein (~3 ng) was added in the VP16-Oct-1-DNA assay. Reaction mixtures were incubated under the same conditions as for the VP16-induced complex assay except that the 3% fetal bovine serum and 0.75  $\mu$ g of poly(dI-dC) were replaced with 100  $\mu$ g of bovine serum albumin and 10 ng of poly(dI-dC). After incubation, reaction mixtures were loaded onto a 6%, 19:1 acrylamide/bisacrylamide 0.25 $\times$  Tris-borate-EDTA gel as described previously (27).

**In vivo VP16 transcriptional activation assay.** Transcriptional activation by influenza virus hemagglutinin epitope-tagged VP16 proteins was assayed in HeLa cells by using the reporter system described previously (3). HeLa cells were seeded at 5  $\times$  10<sup>5</sup> cells per 10-cm-diameter plate and transfected after 24 h by

calcium phosphate coprecipitation (30). In those cells where wild-type or mutant VP16 proteins were expressed, 1  $\mu$ g of wild-type or mutant pCGNVP16 expression vector was cotransfected. RNA preparation and measurement of RNA expression by RNase protection were done essentially as described previously (20). Expression of the epitope-tagged VP16 proteins was measured by immunoblot analysis with monoclonal antibody 12CA5.

## RESULTS

**Experimental design.** Figure 1 shows a schematic of VP16, indicating regions involved in VP16-induced complex formation and transcriptional activation. Below the illustration of VP16 is shown the amino acid sequence of the entire activation domain-proximal region analyzed here. To study the structure and function of this region, we substituted an extensive set of individual and combined amino acids with alanines and assayed each mutant's activity in four separate in vitro assays: (i) VP16-induced complex formation, (ii) VP16 binding to HCF, (iii) VP16 binding to DNA, and (iv) VP16 binding to an Oct-1-DNA complex.

Table 1 lists all of the VP16 mutants studied here. We substituted all of the charged residues in the region (residues 331 to 391) for alanine, either individually or in combination, because charged residues are more likely to be exposed on the surface of VP16 (5, 6) and thus involved in macromolecular interactions. In one particular region (residues 373 to 375), we also substituted uncharged residues for alanine because these particular amino acids had been shown previously to be important for VP16-induced complex formation (9).

The alanine substitution mutants are referred to as follows. Mutants with a single amino acid substitution are referred to by the identity of the wild-type amino acid, followed by its position in VP16 and the identity of the missense mutation (e.g., exchange of the arginine residue at position 331 of VP16 for alanine is referred to as R331A). Mutants in which two or three consecutive charged residues were simultaneously substituted with alanine are referred to by the position of the amino-terminal exchanged residue followed by "Ala" and the number of mutated residues (e.g., the mutant in which arginine 360 and glutamic acid 361 were replaced by alanine is called 360Ala2 [Table 1]). For comparison, we also analyzed three previously described four-amino-acid insertion mutants, 335i, 368i, and 379i, that have been shown to disrupt VP16-induced complex formation (1, 35) and, in one case (379i), to disrupt selectively VP16 interaction with Oct-1 bound to a TAATGARAT site (27).

Below, we first describe the activities of a selected set of mutants (R331A, 360Ala2, 366Ala3, G374A, E378A, 385Ala3, and 390Ala2) in each of the four in vitro assays. Except for two exceptional mutants (mutants 335i and K343A were expressed exceptionally poorly in *E. coli* and were inactive in all assays, suggesting a gross disruption of VP16 structure), the selected set of mutants is representative of all of the different kinds of activities that we have detected with the mutants analyzed in

TABLE 1. Phenotypes associated with amino acid substitutions in VP16<sup>a</sup>

Insertion or substitution	VP16-induced complex formation	Interaction with:		
		HCF	DNA	Oct-1-DNA
Wild type	++	++	++	++
Insertions				
335i <sup>b</sup>	-	-	-	-
368i	+	+	+/-	+
379i	-	++	++	-
Substitutions				
R331A	-	++	-	-
R341A	+	++	-	+
K343A <sup>b</sup>	-	-	-	-
D345A	++	++	++	++
341Ala3	-	++	-	-
E356A	++	++	++	++
R360A	+	++	+/-	+
E361A	+	+/-	+++	+++
360Ala2	+/-	+/-	+/-	+
R366A	+	++	+/-	+
R368A	+	++	+/-	+
K370A	+	++	+/-	+
366Ala3	-	++	-	-
Y373A	-	++	++	-
G374A	-	++	++	-
S375A	-	++	++	-
E378A	-	++	++	++
D382A	++	++	++	++
385Ala3	+	+	+++	+++
E361A/385Ala3	-	-	++++	++++
390Ala2	++	++	++	++

<sup>a</sup> Wild-type VP16 activity is set at ++ for each assay. +++ and +++++, more active than wild-type VP16; +, less active than wild-type VP16; +/-, barely detectable activity; -, undetectable activity.

<sup>b</sup> Expressed poorly and had probably sustained a gross disruption in structure.

this study. Table 1 summarizes the activities of all of the VP16 mutants studied here. The assays described below are not direct quantitative measurements of protein-protein or protein-DNA affinity, and therefore we indicate only approximate activities in Table 1.

**Numerous VP16 residues located near the VP16 transcriptional activation domain affect VP16-induced complex formation.** Figure 2 shows the abilities of the selected set of VP16 mutants to form a VP16-induced complex on a TAATGARAT site. For this and the other TAATGARAT site-dependent assays, we used a TAATGARAT site originating from the ICP0 promoter that contains an overlapping octamer binding site for Oct-1 (in boldface): **ATGCTAATGATAT**. We refer to this type of TAATGARAT site as (OCTA<sup>+</sup>)TAATGARAT. As expected, at the relatively low levels of VP16 used in this assay, wild-type VP16 does not bind to the (OCTA<sup>+</sup>)TAATGARAT site by itself (Fig. 2; compare lanes 1 and 2). A fractionated HeLa cell extract enriched for Oct-1 and HCF activities (37) generates an Oct-1-DNA complex alone (lane 3; labeled Oct-1) and a slower-migrating VP16-induced complex (labeled VIC) in the presence of VP16 (lane 4).

Of the seven mutants assayed in Fig. 2, four severely disrupted complex formation (R331A, 366Ala3, G374A, and E378A;

lanes 5 and 7 to 9), one had no evident effect (390Ala2; lane 11), and two had intermediate (360Ala2; lane 6) to weak (385Ala3; lane 10) effects. Mutants 385Ala3 and 390Ala2 probably straddle the carboxy-terminal boundary of the region involved in VP16-induced complex formation, because Greaves and O'Hare (9) showed that deletion of carboxy-terminal residues up to amino acid 388 does not affect VP16-induced complex formation, but further deletion does affect complex formation. The disruption of VP16 activity by many individual alanine substitutions throughout the region of VP16 analyzed here (12 of 15 [Fig. 2 and Table 1]) indicates that the entire region is involved in VP16-induced complex formation.

**An electrophoretic mobility retardation assay for DNA-independent protein-protein association.** We next assayed the effects of the mutations on VP16 association with HCF. VP16 association with HCF is independent of DNA (15, 18, 27, 40) and can be assayed by protein affinity precipitation (27, 40). Because this assay is relatively insensitive and tedious, we developed an electrophoretic mobility retardation assay that is simple and sensitive for measuring protein association. In this assay, the target protein is tagged with a DNA-binding domain such that the resulting fusion protein binds DNA specifically in an electrophoretic mobility retardation assay. Protein association is subsequently measured by the ability of a second protein(s) to alter the mobility of the DNA-binding domain-tagged protein bound to DNA in the electrophoretic mobility retardation assay. Here, we fused VP16 to the GAL4 DNA-binding domain (residues 1 to 94) and assayed the binding of

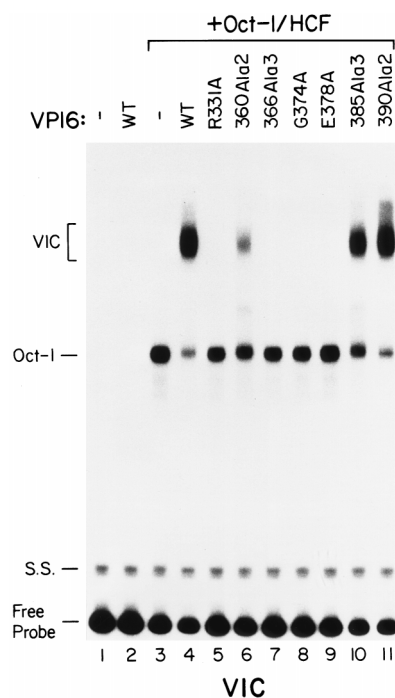


FIG. 2. Some but not all alanine substitutions within VP16 residues 331 and 391 affect VP16-induced complex formation in vitro. An electrophoretic mobility retardation assay for VP16-induced complex formation was performed. The identity of the amino acid exchange(s) for each VP16 mutant is indicated above each lane. All samples contained the (OCTA<sup>+</sup>)TAATGARAT probe, either alone (lane 1) or with VP16 (lane 2), with Oct-1 and HCF (lane 3), or with wild-type (WT; lane 4) or mutant (lanes 5 to 11) VP16 proteins in the presence of Oct-1 and HCF. The positions of the free (OCTA<sup>+</sup>)TAATGARAT probe (Free Probe), denatured single-stranded probe (S.S.), Oct-1-DNA complex (Oct-1), and VP16-induced complexes (VIC) are shown at the left.



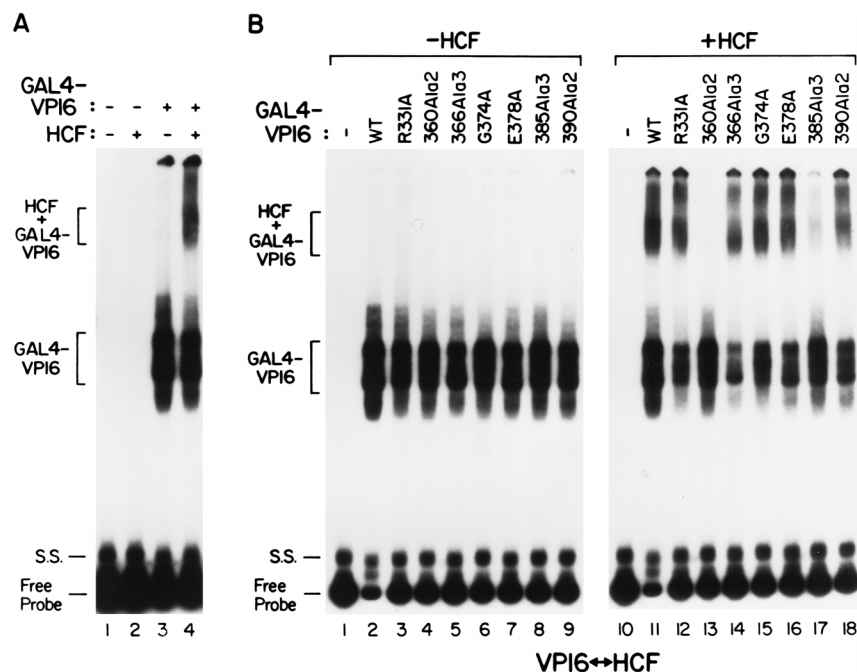


FIG. 3. An electrophoretic mobility retardation assay for DNA-independent protein-protein association reveals VP16 residues involved in binding HCF. (A) Electrophoretic mobility retardation assay with GAL4 DNA-binding domain-tagged VP16. HCF interaction with VP16 was measured by eliciting an alteration in the mobility of a wild-type (WT) GAL4-VP16 fusion protein bound to the GAL4 DNA-binding site. Samples were probe alone (lane 1) or with HCF (lane 2), with GST-GAL4-VP16 $\Delta$ C (lane 3), or with HCF and GST-GAL4-VP16 $\Delta$ C (lane 4). HCF was provided by the WGA Oct-1+HCF HeLa cell fraction; under the conditions of this assay, the Oct-1 in the Oct-1+HCF fraction does not bind to the GAL4-binding site probe or the GAL4-VP16 fusion protein. The positions of the GAL4-binding site probe (Free Probe), denatured single-stranded probe (S.S.), GAL4-VP16-DNA complex (GAL4-VP16), and the multiprotein-DNA complex of HCF, GAL4-VP16, and DNA (HCF + GAL4-VP16) are shown at the left. (B) Effects of amino acid substitutions in VP16 on the interaction with HCF. A GAL4 DNA-binding domain-tagged VP16 electrophoretic mobility retardation assay for VP16-HCF interaction was performed as for panel A with the VP16 alanine-substituted mutants identified above the lanes. GAL4-VP16 fusion proteins were assayed in the absence (lanes 2 to 9) or presence (lanes 11 to 18) of HCF. Lanes 1 and 10, GAL4-binding site probe alone (lane 1) or with HCF (lane 10). The positions of the different electrophoretic species are as described for panel A.

HCF to the hybrid GAL4-VP16 protein bound to a high-affinity GAL4-binding site.

Figure 3A shows the results of such an assay. As expected, on its own, the GAL4-VP16 fusion protein (lane 3), but not HCF (lane 2), bound the GAL4 DNA-binding site effectively. Curiously, the hybrid GAL4-VP16 protein formed a heterogeneous banding pattern. We suspect that this banding pattern is related to the structure of VP16 because other hybrid GAL4 fusion proteins form a single complex (see, for example, reference 31) and because the two VP16 mutants with potentially disrupted structures, 335i and K343A, also form a single homogeneous complex. In any case, addition of HCF resulted in induction of a new complex of slower mobility (lane 4), which is dependent on the VP16 sequences in the GAL4-VP16 fusion (see the VP16 mutant analysis described below). Therefore, this electrophoretic mobility retardation assay serves as an assay for VP16 binding to HCF. In principle, DNA-binding domain tagging together with an electrophoretic mobility retardation assay can be used generally to assay stable protein-protein association.

**Some VP16 mutants defective for VP16-induced complex formation are defective for binding to HCF.** To assay the effects of the VP16 mutations on HCF binding, we transferred the mutations to the GAL4-VP16 fusion protein and assayed the activities of the mutated DNA-binding domain-tagged VP16 proteins in the electrophoretic mobility retardation assay. Figure 3B shows the effects of the set of VP16 mutations assayed in Fig. 2 on the binding to HCF. In the absence of HCF (lanes 1 to 9), the wild-type and mutant GAL4-VP16 fusion proteins display similar DNA-binding patterns. In the

presence of HCF (lanes 10 to 18), however, two of the VP16 mutants, the double-alanine-substitution mutant 360Ala2 (lane 13) and, to a lesser extent, the triple-substitution mutant 385Ala3 (lane 17), display reduced levels of HCF binding. In contrast, the 390Ala2 mutant, which formed the VP16-induced complex normally, and mutants R331A, 366Ala3, G374A and E378A, which were defective for VP16-induced complex formation (Fig. 2), bound HCF at or near wild-type levels (compare lane 11 with lanes 12, 14 to 16, and 18). Together with the VP16-induced complex formation results, the HCF binding results (Table 1) indicate that in the 331 to 391 region of VP16, sequences involved in HCF binding are interdigitated with sequences that are required for some aspect of VP16-induced complex formation other than HCF binding. To investigate these other aspects of VP16-induced complex formation, we studied VP16 association with DNA, either alone or together with Oct-1, in the absence of HCF.

**DNA binding by mutant VP16 proteins in the presence and absence of Oct-1.** At a high concentration, VP16 can bind DNA alone in an electrophoretic mobility retardation assay; in the presence of Oct-1, a lower concentration of VP16 is required to detect DNA binding (27). Figure 4 shows the effects of the selected set of mutations on the ability of VP16 to bind DNA on its own (Fig. 4A) or cooperatively with Oct-1 (Fig. 4B). At the high concentrations of VP16 used in the VP16-only assay, VP16 binds to the DNA probe (Fig. 4A; compare lanes 1 and 2). Two of the VP16 mutants assayed, the single-alanine-substitution mutant R331A (lane 3) and the triple-substitution mutant 366Ala3 (lane 5), are defective for DNA binding on their own. In contrast, the apparently wild-type 390Ala2 mu-

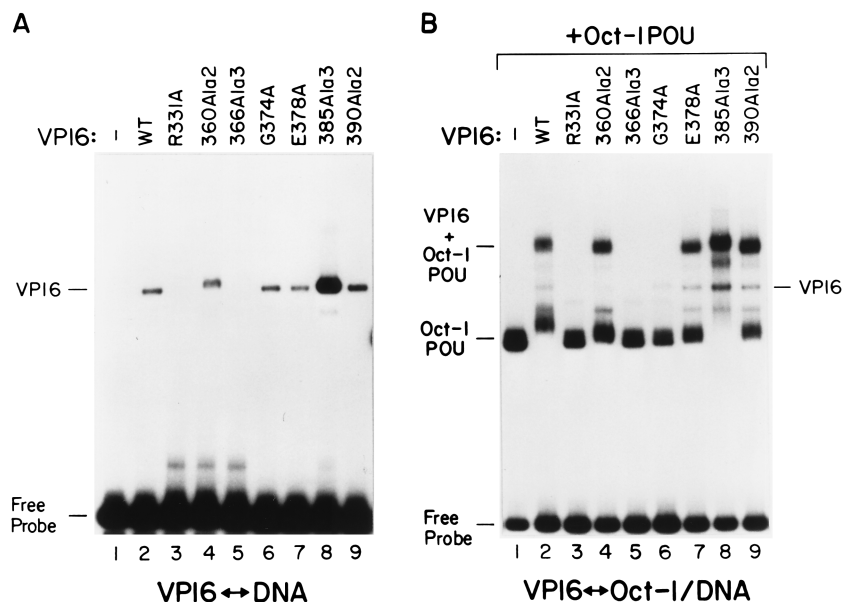


FIG. 4. Effects of VP16 amino acid substitutions on VP16 binding to DNA alone or cooperatively with Oct-1. (A) VP16 binding to DNA alone at a high VP16 concentration. The (OCTA<sup>+</sup>)TAATGARAT probe was incubated either without (lane 1) or with (lanes 2 to 9) wild-type (WT) and mutant GST-VP16 proteins as indicated above the lanes and analyzed on a 6% acrylamide gel as described in Materials and Methods. (B) VP16 binding to DNA cooperatively with the Oct-1 POU domain at an intermediate VP16 concentration. The (OCTA<sup>+</sup>)TAATGARAT probe was incubated with the GST-Oct-1 POU domain fusion protein and either without (lane 1) or with (lanes 2 to 9) wild-type and mutant GST-VP16 proteins as indicated above the lanes. The positions of the free (OCTA<sup>+</sup>)TAATGARAT probe (Free Probe), Oct-1 POU domain-DNA complex (Oct-1 POU), VP16-DNA complex (VP16), and the multiprotein-DNA complex of VP16, Oct-1 POU domain, and DNA (VP16 + Oct-1 POU) are indicated. The gel in panel A is from a longer exposure of the same electrophoretic mobility retardation assay shown in panel B.

tant (lane 9) and mutants 360Ala2, G374A, and E378A (lanes 4, 6, and 7), which were defective for VP16-induced complex formation (Fig. 2), bound DNA on their own at or near wild-type levels. Curiously, the 385Ala3 mutant, which binds HCF with reduced efficiency (Fig. 3B), bound DNA better on its own than did wild-type VP16 (compare lanes 2 and 8). The contrasting abilities of the R331A and 366Ala3 mutant VP16 proteins to bind HCF, but not DNA, and of the 360Ala2 and 385Ala3 mutant VP16 proteins to bind DNA, but not HCF, suggests that different nearby surfaces of VP16 are used to bind HCF and DNA, and that these interactions are not strictly dependent on one another.

Figure 4B shows the effects of the mutations on VP16 binding to the (OCTA<sup>+</sup>)TAATGARAT site cooperatively with the Oct-1 POU domain. We have previously shown that this assay is specific for the Oct-1 POU domain (VP16 does not recognize the closely related Oct-2 POU domain in this assay) and requires the GARAT element of the TAATGARAT sequence (27). In this assay, the Oct-1 POU domain binds DNA on its own (lane 1), and addition of wild-type VP16 induces a VP16-Oct-1 POU domain complex (lane 2); a less abundant complex of intermediate mobility in lane 2 is a VP16-only complex, which may result from decay of the VP16-Oct-1 POU domain complex. VP16-binding assays with purified Oct-1 POU domain showed that the GST moiety in the GST-Oct-1 POU domain fusion proteins used here did not influence VP16 binding to DNA cooperatively with Oct-1 (data not shown).

Except for one mutant, G374A, the same mutants that could bind DNA on their own also bound DNA cooperatively with the Oct-1 POU domain (compare lanes 4 and 7 to 9 in Fig. 4A and B), and the two VP16 mutants that failed to bind DNA effectively on their own also failed to bind cooperatively with Oct-1 (compare lanes 3 and 5 in Fig. 4A and B). Significantly, the HCF-binding-defective mutant 385Ala3, which bound DNA on its own better than wild-type VP16, also formed the

VP16-Oct-1 POU domain complex better than wild-type VP16 (compare lanes 2 and 8), suggesting that VP16 binds DNA on its own in a manner similar to how it binds DNA cooperatively with Oct-1.

From among this set of VP16 mutants, the mutant G374A displayed a unique phenotype: it binds DNA on its own with wild-type affinity but fails to bind DNA cooperatively with the Oct-1 POU domain (compare lanes 6 in Fig. 4A and B). Substitution of the flanking residues in mutants Y373A and S375A displays the same phenotype (Table 1 [the effect of S375A on cooperative binding with Oct-1 has also been described by Walker et al. {34}; Oct-1-independent binding to DNA was not assayed in that study]). The Oct-1 association-specific defect of these mutants is identical to that previously described for the neighboring 379i insertion mutant (27) (Table 1). These results suggest that this region of VP16 (residues 373 to 379) interacts with the Oct-1 POU domain, probably the POU homeodomain, and not other components of the VP16-induced complex.

Together, the analysis of the selected set of VP16 mutants reveals that interactions with Oct-1, HCF, and DNA are interdigitated within this small region of VP16; indeed, separate residues within a region as small as 13 amino acids (residues 361 to 373 [Table 1; see also below]) are involved in association with either Oct-1, HCF, or DNA. One mutant, E378A, is of particular interest: it is defective for formation of the VP16-induced complex (Fig. 2) but displayed no evident defect in binding to HCF, to DNA, or to DNA cooperatively with Oct-1 (Fig. 3 and 4).

**Adjacent VP16 residues are separately involved in HCF and DNA binding.** Because the HCF-binding-defective VP16 mutant 360Ala2 is mutated in adjacent basic (arginine) and acidic (glutamic acid) residues, we were interested in determining which, if not both, of these two residues is involved in HCF binding. Figure 5 shows the effects of each alanine substitution on VP16-induced complex formation (Fig. 5A) and on binding

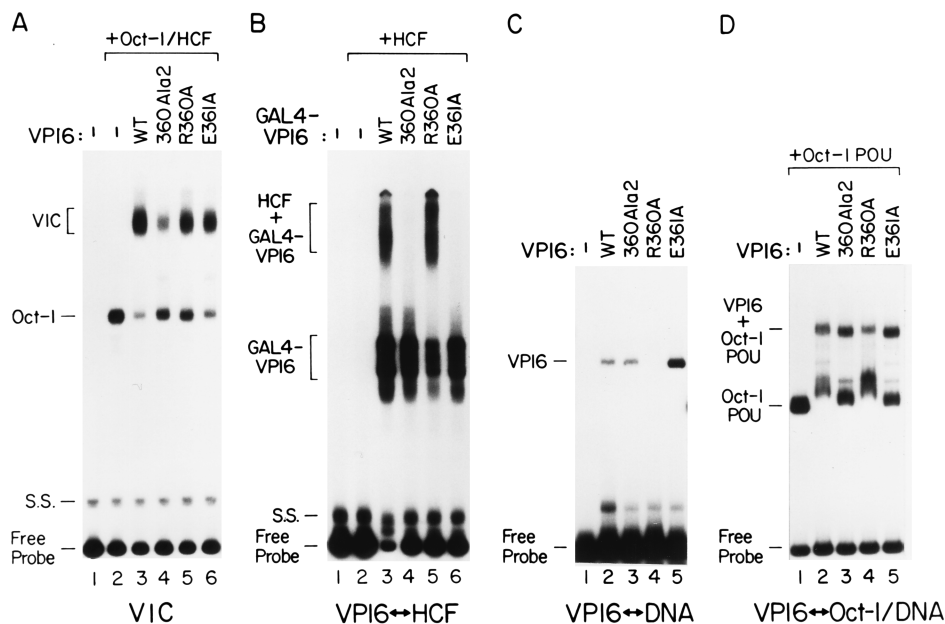


FIG. 5. Two adjacent VP16 residues, R360 and E361, are involved in DNA and HCF interaction, respectively. Wild-type and mutant (360Ala2, R360A, and E361A) VP16 molecules were tested for VP16-induced complex formation (A) and for individual interaction with HCF (B), DNA (C), or DNA with Oct-1 (D). (A) VP16-induced complex formation was assayed as for Fig. 2. The presence or absence of wild-type (WT) or mutant VP16 and of the Oct-1+HCF fraction is indicated above the lanes. (B) VP16 binding to HCF was assayed by electrophoretic mobility retardation as described for Fig. 3. The presence or absence of wild-type (WT) or mutant GAL4-VP16 fusion protein and of the HCF-containing fraction is indicated above the lanes. (C) VP16 binding to DNA alone was assayed as for Fig. 4A. The presence or absence of wild-type (WT) or mutant VP16 is indicated above the lanes. (D) VP16 binding to DNA cooperatively with Oct-1 was assayed as for Fig. 4B. The presence or absence of wild-type (WT) or mutant VP16 and of GST-Oct-1 POU domain fusion protein is indicated above the lanes. The positions of the different electrophoretic species are as described in the legends to Fig. 2 to 4.

to HCF (Fig. 5B), to DNA (Fig. 5C), and to DNA cooperatively with Oct-1 (Fig. 5D). Both of the individual amino acid substitutions, R360A and E361A, are only slightly defective for VP16-induced complex formation compared to the parental double-substitution mutant 360Ala2 (Fig. 5A; compare lanes 3 and 4 with lanes 5 and 6), suggesting that both residues are involved in VP16-induced complex formation.

When assayed for binding to HCF, however, the E361A mutant, but not the R360A mutant, was defective (Fig. 5B; compare lanes 3 to 6), whereas when assayed for binding to DNA alone (Fig. 5C) and to a lesser extent cooperatively with Oct-1 (Fig. 5D), the R360A mutant, but not the E361A mutant, was defective (compare lanes 2 to 5). Indeed, like the other HCF-binding defective mutant 385Ala3, the E361A mutant displays improved binding to DNA on its own (Fig. 5C; compare lanes 2 and 5). These results show that adjacent residues in VP16 are involved in different functions, interaction with DNA (R360) or with HCF (E361), and that, remarkably, disruption of one activity does not necessarily disrupt the other; indeed, substitution of E361 only improves DNA binding. The positive effect of the E361A mutation on DNA binding may explain why, even though the R360A mutant is defective for DNA binding (although some DNA-binding activity is evident in longer exposures [Table 1]), the combined R360A/E361A double mutant (360Ala2) is not defective for DNA binding (Fig. 5C, lane 3). Although we have no direct evidence that these residues of VP16 contact either HCF or DNA, the surprisingly contrasting effects of these two adjacent substitutions suggest that VP16, HCF, and the DNA are in close proximity in the VP16-induced complex.

**A combination of mutations defective for HCF binding increases HCF-independent VP16 association with Oct-1 and DNA.** Curiously, both of the mutants that are defective for

HCF binding, E361A and 385Ala3, displayed increased binding to DNA. We therefore tested the combined effects of these two mutations in a mutant called E361A/385Ala3, as shown in Fig. 6. Compared to the individual mutations, which have a relatively small effect on VP16-induced complex formation, the combined mutant E361A/385Ala3 is very defective for VP16-induced complex formation (Fig. 6A; compare lanes 3 to 6), although it may form an HCF-independent VP16-induced complex (Fig. 6A, lane 6). In the assays for the individual VP16 interactions, E361A/385Ala3 is defective for HCF binding (Fig. 6B, compare lanes 3 to 6) and now binds DNA on its own even better than the individual mutants (Fig. 6C; compare lanes 2 to 6). Separate experiments showed that the combined E361A/385Ala3 mutant also binds DNA cooperatively with Oct-1 better than the individual mutants (data not shown; this effect cannot be seen in Fig. 6D because the Oct-1-DNA complex has already been depleted in the 385Ala3 binding reaction [compare lanes 4 and 5]). Thus, the E361A/385Ala3 mutant fails to associate with HCF but exhibits the highest affinity for Oct-1 bound to a TAATGARAT site in the absence of HCF.

**VP16 mutants defective for interaction with HCF, DNA, or Oct-1 are defective for transcriptional activation in vivo.** To understand the requirements for VP16 activation of transcription in vivo, we assayed the abilities of selected VP16 mutants to activate transcription in human cells. Figure 7 shows the results of VP16-dependent transcriptional activation of a  $\beta$ -globin promoter containing multimerized TAATGARAT sites (3) after transient expression of wild-type and mutant VP16 in HeLa cells. Eight different VP16 mutants were assayed. They represent mutants defective in HCF binding (360Ala2, E361A, 385Ala3, and E361A/385Ala3), DNA binding (R360A and 366Ala3), or Oct-1 association (G374A) and

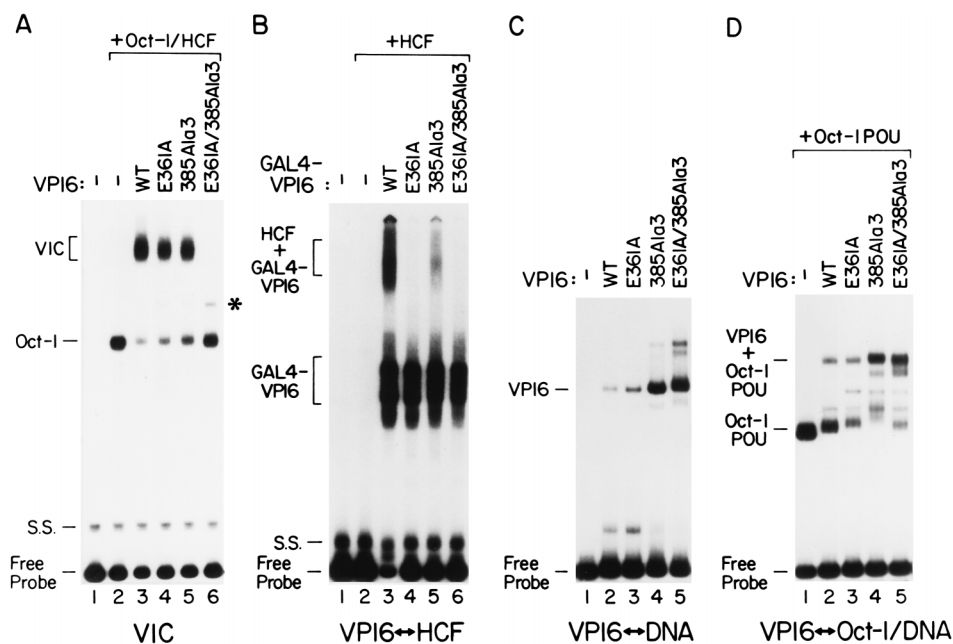


FIG. 6. The VP16 mutant E361A/385Ala3 is defective for HCF association but possesses an increased affinity for DNA in the absence or presence of Oct-1. Wild-type, E361A, 385Ala3, and E361A/385Ala3 VP16 molecules were tested for VP16-induced complex formation (A) and for individual interaction with HCF (B), DNA (C), or DNA with Oct-1 (D). (A) VP16-induced complex (VIC) formation was assayed as for Fig. 2. The presence or absence of wild-type (WT) or mutant VP16 and of the Oct-1+HCF fraction is indicated above the lanes. The asterisk indicates the position of a likely HCF-independent VP16-induced complex. (B) VP16 binding to HCF was assayed by electrophoretic mobility retardation as described for Fig. 3. The presence or absence of wild-type (WT) or mutant GAL4-VP16 fusion protein and of the HCF-containing fraction is indicated above the lanes. (C) VP16 binding to DNA alone was assayed as for Fig. 4A. The presence or absence of wild-type (WT) or mutant VP16 is indicated above the lanes. (D) VP16 binding to DNA cooperatively with Oct-1 was assayed as for Fig. 4B. The presence or absence of wild-type (WT) or mutant VP16 and of GST-Oct-1 POU domain fusion protein is indicated above the lanes. The positions of the different electrophoretic species are as described in the legends to Fig. 2 to 4.

the one mutation, E378A, which is very defective for VP16-induced complex formation but displays no defect for any individual VP16 interaction (Table 1). Immunoblot analysis showed that all of these VP16 proteins are stably expressed at similar levels (data not shown).

As expected, transcriptional activity of the reporter construct was dependent on the presence of VP16 (Fig. 7; compare lane 1 with lanes 2 and 11). The effects of the mutations on activation of the promoter *in vivo* closely parallel the abilities of the mutant proteins to form a VP16-induced complex *in vitro*. Thus, the four mutants that do not form a VP16-induced complex *in vitro* (366Ala3, G374A, E378A, and E361A/385Ala3) displayed no evident activity *in vivo* (Fig. 7, lanes 6 to 8 and 10). In contrast, of the four mutants that displayed some VP16-induced complex formation activity *in vitro* (360Ala2, R360A, E361A, and 385Ala3), two displayed evident activity *in vivo* (lanes 4 and 9), and the two others (lanes 3 and 5) displayed very weak activity, which was evident only in long exposures. These results suggest that VP16-induced complex formation assayed *in vitro* reflects the requirements for complex formation and transcriptional activation *in vivo* and that interactions with HCF, DNA, and Oct-1 are all important for VP16 to activate transcription *in vivo*.

## DISCUSSION

We have used mutagenesis to measure the contribution of VP16 residues located near its transcriptional activation domain (residues 331 to 391) for formation of the VP16-induced complex. By assaying mutant VP16 molecules for individual activities associated with VP16-induced complex formation (i.e., interaction with Oct-1, HCF, and DNA), we have sepa-

rated the contributions of individual residues for these different activities. Figure 8 displays the different effects of the various mutations below the sequence of the activation domain-proximal region of VP16. The mutations have been divided into four categories: those that disrupt the three individual activities of VP16 (binding to HCF, binding to DNA alone,

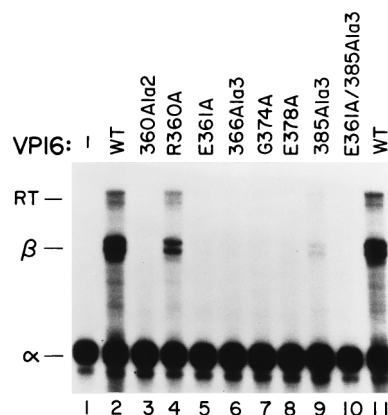


FIG. 7. *In vivo* transcriptional activation by VP16 amino acid substitution mutants. The  $\beta$ -globin reporter plasmid and  $\alpha$ -globin internal reference plasmid were transfected into HeLa cells in either the absence (lane 1) or presence (lanes 2 to 11) of wild-type (WT) or mutant VP16 expression plasmid, and RNA expression was analyzed by RNase protection as described in Materials and Methods. Bands corresponding to correctly initiated  $\alpha$ -globin ( $\alpha$ ) and  $\beta$ -globin ( $\beta$ ) transcripts and incorrect  $\beta$ -globin readthrough (RT) transcripts are indicated. Samples were adjusted (no more than  $\pm$  two- to threefold) to equalize the  $\alpha$ -globin signal. Similar results were obtained in three experiments.



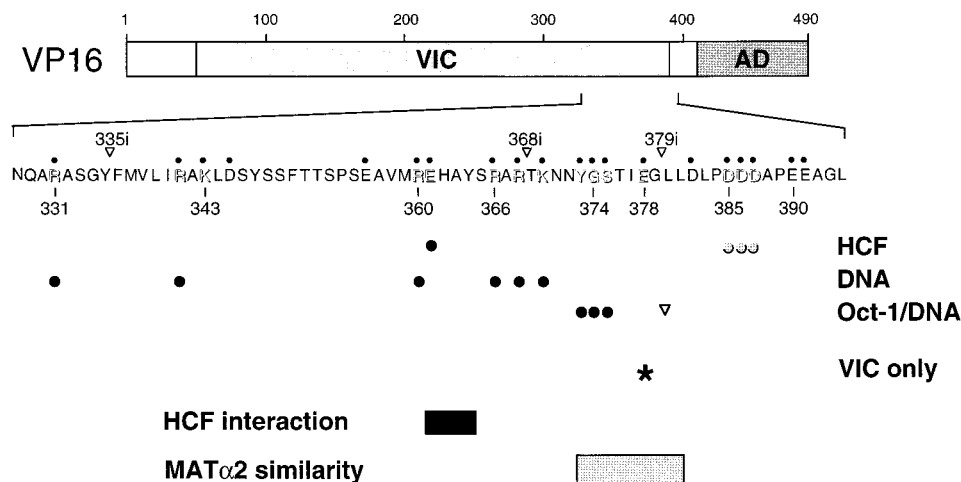


FIG. 8. Interdigitated residues within a small region of VP16 interact with Oct-1, HCF, and DNA. The illustration of VP16 and the identification of substituted residues are as shown in Fig. 1. Residues whose replacement by alanine disrupts VP16-induced complex (VIC) formation are highlighted in the sequence. Loss of VP16 binding to HCF (HCF), DNA alone (DNA), or exclusively DNA with Oct-1 (Oct-1/DNA) is indicated by a black dot for substitutions and a triangle for insertions below each respective site; two mutants that were defective for all activities, 335i and K343A, are not included in the display below the sequence. The effect of the 385Ala3 mutation of HCF binding is indicated by shaded dots to indicate that substitution of these three aspartic acid residues was not assayed individually. The position of the unusual mutant E378A, which is only defective for formation of the complete VP16-induced complex (VIC only), is shown by the asterisk. The positions of the EHAY sequence implicated in HCF interaction by peptide competition (39) and the MAT $\alpha$ 2 sequence similarity (21) are shown at the bottom.

and binding to the Oct-1-DNA complex but not to DNA alone) and the one mutation, E378A, which is defective for VP16-induced complex formation but possesses all of the individual VP16 activities. The pattern of effects of the mutations suggests that the different activities of VP16 involved in formation of the VP16-induced complex are separable except for the ability to bind DNA cooperatively with Oct-1, which appears dependent on the DNA-binding activity of VP16.

Because the VP16-induced complex contains multiple components, it has been difficult to ascertain which of the components of the VP16-induced complex are directly contacted by VP16. In particular, the issue of whether VP16 contacts DNA is controversial: although VP16 can bind DNA on its own, O'Hare and colleagues have suggested that, rather than contact DNA, VP16 associates with a specific binding site-induced conformation of the Oct-1 POU domain (22, 34). Our results, however, argue that VP16 does bind DNA in the VP16-induced complex and that it does so in a manner similar to how it binds DNA alone: in every instance where a mutation either disrupted or enhanced VP16 binding to DNA alone, the mutation had a similar effect on VP16 binding to DNA cooperatively with Oct-1 (Table 1). If VP16 did not bind DNA in the VP16-induced complex as it does on its own, there would be no reason for the effects of mutations on VP16 binding to DNA alone and with Oct-1 to correspond to each other. For this and other reasons (14), we therefore continue to favor the hypothesis that VP16 makes direct and sequence-specific contacts with DNA (13).

Residues whose substitution affects HCF binding are located in two separate regions of VP16, residue E361 and one or more of residues D385, D386, and D387; these positions flank substitutions that affect DNA and Oct-1 interaction (Fig. 8). Residue E361 has been previously implicated in interaction with HCF: peptides corresponding to this region of VP16 can inhibit VP16-induced complex formation, probably by preventing VP16 binding to HCF (10, 11, 39), and alanine substitution of residue E361 and two neighboring residues (H362 and Y364) in such synthetic peptides disrupts the ability of these peptides to inhibit VP16-induced complex formation (39) (bot-

tom of Fig. 8). These three residues lie between residues involved in DNA binding (indeed, residue E361 is immediately adjacent to residue R360, which is involved in DNA binding), suggesting that HCF lies near the DNA in the VP16-induced complex. The proposed proximity of the HCF-interacting residues of VP16 with DNA may explain the curious result that substitution of HCF-interacting residues for alanine increases the association of VP16 with DNA on its own (Fig. 6). The HCF-interacting residues that we have substituted are all acidic, and these residues may clash with nearby phosphates in the DNA. Indeed, perhaps one way HCF can promote VP16-induced complex formation is by masking the negative charge of these acidic VP16 residues.

Many of the substitutions that affect VP16-induced complex formation affect VP16 binding to DNA on its own. Consistent with interaction with negatively charged DNA, substitution of basic residues in this region affected VP16 binding to DNA on its own or cooperatively with Oct-1 but not to HCF (Table 1). These results differ from those of Shaw et al. (26), who studied the activity of individual alanine substitution of residues R360, R366, R368, and K370 and found that only substitution of residues R360 and R366 affected DNA binding on its own; substitution of three residues, R366, R368, and K370, affected binding to HCF. In light of our results, the latter result is surprising, because even when we combine all three of these substitutions in the mutant 366Ala3, we observed at most a very minor effect on HCF interaction (Fig. 3).

In a further contrast to the studies of Shaw et al. (26), we find that mutations that affect individual activities of VP16 also affect VP16-induced complex formation *in vitro* and activation of transcription *in vivo*. We therefore conclude that interaction with each of the three other components of the VP16-induced complex, DNA, Oct-1, and HCF, is important for VP16 activation of transcription *in vivo*. Consistent with the hypothesis that VP16 interaction with HCF is important for activation of transcription by VP16, VP16 fails to activate transcription at nonpermissive temperature in a cell line carrying a temperature-sensitive mutation in HCF that disrupts VP16-induced complex formation at the nonpermissive temperature (7).



Lastly, our results substantiate a hypothesis proposed by Li et al. (21) suggesting that VP16 interacts with the Oct-1 homeodomain in a manner analogous to the interaction of the yeast protein MAT $\alpha$ 2 with the homeodomain of MATA1. MAT $\alpha$ 2 and MATA1 are two homeodomain proteins which form a highly cooperative heterodimeric complex on DNA; cooperative binding is mediated by a carboxy-terminal tail in MAT $\alpha$ 2 which in the absence of MATA1 is unstructured but when complexed to MATA1 becomes structured, forming a short  $\alpha$  helix that contacts the MATA1 homeodomain (21). The MAT $\alpha$ 2 tail interacts with the same surface of the MATA1 homeodomain as the one VP16 interacts with on the Oct-1 homeodomain (24), and Li et al. (21) noted a short segment of sequence similarity between MAT $\alpha$ 2 and VP16 (bottom of Fig. 8) in the region of VP16 shown to be involved in Oct-1 interaction (27). In this study, we identified three additional residues that selectively affect VP16 binding cooperatively to DNA with Oct-1, and they all lie within this proposed region of MAT $\alpha$ 2 similarity (residues 373 to 375), substantiating the significance of the proposed analogy between MAT $\alpha$ 2 and VP16 (21).

Taken together, the analogy to the MATA1-MAT $\alpha$ 2 complex and the results presented here suggest a model for the structure of the VP16-induced complex: the region of MAT $\alpha$ 2 similarity in VP16 interacts with the Oct-1 homeodomain, and, as in MAT $\alpha$ 2, the VP16 sequences immediately amino terminal of the MAT $\alpha$ 2 similarity interact with the DNA. Consistent with this model, VP16 residues amino terminal of the MAT $\alpha$ 2 similarity are involved in DNA binding (Fig. 8). In this model, the sites of HCF interaction with VP16 flank the critical DNA-Oct-1 homeodomain interaction region of VP16: residues 361 to 364 lie amino terminal of the DNA-contacting residues, and residues 385 to 387 lie carboxy terminal of the Oct-1 interaction region. Perhaps HCF stabilizes the VP16-induced complex by stabilizing the structure of VP16 in the conformation that is favorable for interaction with Oct-1 and a TAATGARAT site. For example, by analogy to MAT $\alpha$ 2 and consistent with the protease sensitivity of this region (11), the region of VP16 that interacts with DNA and Oct-1 may be unstructured on its own and HCF might induce formation of an  $\alpha$  helix in VP16 that promotes interaction with Oct-1. In this model, the Oct-1 interaction region of VP16 might become sandwiched between HCF and the Oct-1 homeodomain.

Such a configuration could explain the very curious phenotype of the E378A mutant, which could perform all of the individual functions of VP16 at wild-type levels but failed to form a complete VP16-induced complex. The E378A substitution lies within the Oct-1 homeodomain interaction region. Perhaps it is only when sandwiched between HCF and Oct-1 in a complete VP16-induced complex that substitution of E378 is deleterious to complex formation.

#### ACKNOWLEDGMENTS

We thank R. Aurora and A. Wilson for reagents; M. Tanaka for suggesting DNA-binding domain tagging; N. Hernandez, A. Stenlund, M. Tanaka, and W. Tansey for critical readings of the manuscript; and J. Duffy and P. Renna for artwork.

This study was supported by PHS grant CA13106 from the National Cancer Institute.

#### REFERENCES

- Ace, C. I., M. A. Dalrymple, F. H. Ramsay, V. G. Preston, and C. M. Preston. 1988. Mutational analysis of the herpes simplex virus type 1 trans-inducing factor Vmw65. *J. Gen. Virol.* **69**:2595-2605.
- Aurora, R., and W. Herr. 1992. Segments of the POU domain influence another's DNA-binding specificity. *Mol. Cell. Biol.* **12**:455-467.
- Cleary, M. A., S. Stern, M. Tanaka, and W. Herr. 1993. Differential positive control by Oct-1 and Oct-2: activation of a transcriptionally silent motif through Oct-1 and VP16 corecruitment. *Genes Dev.* **7**:72-83.
- Cousens, D. J., R. Greaves, C. R. Goding, and P. O'Hare. 1989. The C-terminal 79 amino acids of the herpes simplex virus regulatory protein, Vmw65, efficiently activate transcription in yeast and mammalian cells in chimeric DNA-binding proteins. *EMBO J.* **8**:2337-2342.
- Gibbs, C. S., and M. J. Zoller. 1991. Identification of electrostatic interactions that determine the phosphorylation site specificity of the cAMP-dependent protein kinase. *Biochemistry* **30**:5329-5334.
- Gibbs, C. S., and M. J. Zoller. 1991. Rational scanning mutagenesis of a protein kinase identifies functional regions involved in catalysis and substrate interactions. *J. Biol. Chem.* **266**:8923-8931.
- Goto, H., S. Motomura, A. C. Wilson, R. N. Freiman, Y. Nakabeppu, K. Fukushima, M. Fujishima, W. Herr, and T. Nishimoto. 1997. A single point mutation in HCF causes temperature-sensitive cell-cycle arrest and disrupts VP16 function. *Genes Dev.* **11**:726-737.
- Greaves, R., and P. O'Hare. 1989. Separation of requirements for protein-DNA complex assembly from those for functional activity in the herpes simplex virus regulatory protein Vmw65. *J. Virol.* **63**:1641-1650.
- Greaves, R., and P. O'Hare. 1990. Structural requirements in the herpes simplex virus type 1 transactivator Vmw65 for interaction with the cellular octamer-binding protein and target TAATGARAT sequences. *J. Virol.* **64**:2716-2724.
- Haigh, A., R. Greaves, and P. O'Hare. 1990. Interference with the assembly of a virus-host transcription complex by peptide competition. *Nature (London)* **344**:257-259.
- Hayes, S., and P. O'Hare. 1993. Mapping of a major surface-exposed site in herpes simplex virus protein Vmw65 to a region of direct interaction in a transcription complex assembly. *J. Virol.* **67**:852-862.
- Heitman, J., J. Treisman, N. G. Davis, and M. Russel. 1989. Cassettes of the fl1 intergenic region. *Nucleic Acids Res.* **17**:4413.
- Herr, W., and M. A. Cleary. 1995. The POU domain: versatility in transcriptional regulation by a flexible two-in-one DNA-binding domain. *Genes Dev.* **9**:1679-1693.
- Huang, C. C., and W. Herr. 1996. Differential control of transcription by homologous homeodomain coregulators. *Mol. Cell. Biol.* **16**:2967-2976.
- Katan, M., A. Haigh, C. P. Verrijzer, P. C. van der Vliet, and P. O'Hare. 1990. Characterization of a cellular factor which interacts functionally with Oct-1 in the assembly of a multicomponent transcription complex. *Nucleic Acids Res.* **18**:6871-6880.
- Kristie, T. M., J. H. LeBowitz, and P. A. Sharp. 1989. The octamer-binding proteins form multi-protein-DNA complexes with the HSV  $\alpha$ TIF regulatory protein. *EMBO J.* **8**:4229-4238.
- Kristie, T. M., J. L. Pomerantz, T. C. Twomey, S. A. Parent, and P. A. Sharp. 1995. The cellular C1 factor of the herpes simplex virus enhancer complex is a family of polypeptides. *J. Biol. Chem.* **270**:4387-4394.
- Kristie, T. M., and P. A. Sharp. 1990. Interactions of the Oct-1 POU subdomains with specific DNA sequences and with the HSV  $\alpha$ -transactivator protein. *Genes Dev.* **4**:2383-2396.
- Kunkel, T. A., J. D. Roberts, and R. A. Zakour. 1987. Rapid and efficient site-specific mutagenesis without phenotypic selection. *Methods Enzymol.* **154**:367-382.
- Lai, J.-S., M. A. Cleary, and W. Herr. 1992. A single amino acid exchange transfers VP16-induced positive control from the Oct-1 to the Oct-2 homeo domain. *Genes Dev.* **6**:2058-2065.
- Li, T., M. R. Stark, A. D. Johnson, and C. Wolberger. 1995. Crystal structure of the MATA1/MAT $\alpha$ 2 homeodomain heterodimer bound to DNA. *Science* **270**:262-269.
- Misra, V., S. Walker, P. Yang, S. Hayes, and P. O'Hare. 1996. Conformational alteration of Oct-1 upon DNA binding dictates selectivity in differential interactions with related transcriptional coactivator. *Mol. Cell. Biol.* **16**:4404-4413.
- O'Hare, P. 1993. The virion transactivator of herpes simplex virus. *Semin. Virol.* **4**:145-155.
- Pomerantz, J. L., T. M. Kristie, and P. A. Sharp. 1992. Recognition of the surface of a homeo domain protein. *Genes Dev.* **6**:2047-2057.
- Sadowski, I., J. Ma, S. J. Triezenberg, and M. Ptashne. 1988. GAL4-VP16 is an unusually potent transcriptional activator. *Nature (London)* **335**:563-564.
- Shaw, P., J. Knez, and J. P. Capone. 1995. Amino acid substitutions in the herpes simplex virus transactivator VP16 uncouple direct protein-protein interaction and DNA binding from complex assembly and transactivation. *J. Biol. Chem.* **270**:29030-29037.
- Stern, S., and W. Herr. 1991. The herpes simplex virus trans-activator VP16 recognizes the Oct-1 homeo domain: evidence for a homeo domain recognition subdomain. *Genes Dev.* **5**:2555-2566.
- Studier, F. W., A. H. Rosenberg, J. J. Dunn, and J. W. Dubendorff. 1990. Use of T7 RNA polymerase to direct expression of cloned genes. *Methods Enzymol.* **185**:60-89.
- Tanaka, M., W. M. Clouston, and W. Herr. 1994. The Oct-2 glutamine-rich and proline-rich activation domains can synergize with each other or duplicate themselves to activate transcription. *Mol. Cell. Biol.* **14**:6046-6055.
- Tanaka, M., U. Grossniklaus, W. Herr, and N. Hernandez. 1988. Activation

- of the U2 snRNA promoter by the octamer motif defines a new class of RNA polymerase II enhancer elements. *Genes Dev.* **2**:1764–1778.
31. **Tanaka, M., and W. Herr.** 1994. Reconstitution of transcriptional activation domains by reiteration of short peptide segments reveals the modular organization of a glutamine-rich activation domain. *Mol. Cell. Biol.* **14**:6056–6067.
  32. **Thompson, C. C., and S. L. McKnight.** 1992. Anatomy of an enhancer. *Trends Genet.* **8**:232–236.
  33. **Triebenberg, S. J., R. C. Kingsbury, and S. L. McKnight.** 1988. Functional dissection of VP16, the trans-activator of herpes simplex virus immediate early gene expression. *Genes Dev.* **2**:718–729.
  34. **Walker, S., S. Hayes, and P. O'Hare.** 1994. Site-specific conformational alteration of the Oct-1 POU domain-DNA complex as the basis for differential recognition by Vmw65 (VP16). *Cell* **79**:841–852.
  35. **Werstuck, G., and J. P. Capone.** 1989. Mutational analysis of the herpes simplex virus trans-inducing factor Vmw65. *Gene* **75**:213–224.
  36. **Wilson, A. C., M. A. Cleary, J.-S. Lai, K. LaMarco, M. G. Peterson, and W. Herr.** 1993. Combinatorial control of transcription: the herpes simplex virus VP16-induced complex. *Cold Spring Harbor Symp. Quant. Biol.* **58**:167–178.
  37. **Wilson, A. C., K. LaMarco, M. G. Peterson, and W. Herr.** 1993. The VP16 accessory protein HCF is a family of polypeptides processed from a large precursor protein. *Cell* **74**:115–125.
  38. **Wilson, A. C., M. G. Peterson, and W. Herr.** 1995. The HCF repeat is an unusual proteolytic cleavage signal. *Genes Dev.* **9**:2445–2458.
  39. **Wu, T. J., G. Monokian, D. F. Mark, and C. R. Wobbe.** 1994. Transcriptional activation by herpes simplex virus type 1 VP16 in vitro and its inhibition by oligopeptides. *Mol. Cell. Biol.* **14**:3484–3493.
  40. **Xiao, P., and J. P. Capone.** 1990. A cellular factor binds to the herpes simplex virus type 1 transactivator Vmw65 and is required for Vmw65-dependent protein-DNA complex assembly with Oct-1. *Mol. Cell. Biol.* **10**:4974–4977.